Received: 18 December 2021 | Revised: 8 February 2022 | Accepted: 5 March 2022

DOI: 10.1111/cbdd.14039

RESEARCH ARTICLE

WILEY

2-Aminothiophene derivatives as a new class of positive allosteric modulators of glucagon-like peptide 1 receptor

Tejashree Redij[1] | **James A. McKee**[2] | **Phu Do**[2] | **Jeffrey A. Campbell**[2] | **Jian Ma**[3] | **Zhiyu Li**[4] | **Nicholas Miller**[2] | **Chananchida Srikanlaya**[2] | **Dianzheng Zhang**[5] | **Xianxin Hua**[3] | **Zhijun Li**[1,2]

[1]Department of Biological Sciences, University of the Sciences in Philadelphia, Philadelphia, Pennsylvania, USA

[2]Department of Chemistry & Biochemistry, University of the Sciences in Philadelphia, Philadelphia, Pennsylvania, USA

[3]Department of Cancer Biology, Diabetes Research Center (DRC), University of Pennsylvania, Philadelphia, Pennsylvania, USA

[4]Department of Pharmaceutical Sciences, University of the Sciences in Philadelphia, Philadelphia, Pennsylvania, USA

[5]Department of Bio-Medical Sciences, Philadelphia College of Osteopathic Medicine, Philadelphia, Pennsylvania, USA

Correspondence
Zhijun Li, Department of Chemistry & Biochemistry, Box 48, University of the Sciences in Philadelphia, Philadelphia, PA 19104, USA.
Email: z.li@usciences.edu

Funding information
University of Pennsylvania Institute for Translational Medicine and Therapeutics; National Institutes of Health

Abstract

We report the discovery of two new 2-aminothiophene based small molecule positive allosteric modulators (PAMs) of glucagon-like peptide 1 receptor (GLP-1R) for the treatment of type 2 diabetes. One of the chemotypes, (**S-1**), has a molecular weight of 239 g/mol, the smallest molecule among all reported GLP-1R PAMs. When combined with GLP-1 peptide, **S-1** increased the GLP-1R activity in a dose-dependent manner in a cell-based assay. When combined with the peptide agonist of vasoactive intestinal polypeptide receptor 1 (VIPR1), **S-1** showed no specific activity on VIPR1, another class B GPCR present in the same HEK293-CREB cell line. Insulin secretion studies found **S-1** combined with GLP-1 increased insulin secretion by 1.5-fold at 5 μM. In a mechanistic study, evidence is provided that the synergistic effect of **S-1** with GLP-1 may be partly due to the enhanced impact on CREB based phosphorylation. Given the favorable profile of these chemotypes, the work reported herein suggests that 2-aminothiophene derivatives are a new and promising class of GLP-1R PAMs.

KEYWORDS

2-aminothiophene, glucagon-like peptide 1 receptor, insulin secretion, positive allosteric modulators, type 2 diabetes

We would like to dedicate this manuscript to the memory of Dr. James McKee, father of Dr. James A. McKee, a long-time medicinal chemist and faculty member at our institution, who passed away in 2021.

1 | INTRODUCTION

The glucagon-like peptide 1 (GLP-1) is an important incretin hormone secreted in the gut in response to food intake and is responsible for glucose homeostasis in plasma. GLP-1 acts on the glucagon-like peptide 1 receptor (GLP-1R) to stimulate glucose-dependent insulin secretion and reduce glucagon secretion (Koole et al., 2013). Given its physiological role, GLP-1R, a member of secretin-like Class B family of G-protein coupled receptors (GPCRs), is an effective target for the therapeutic treatment of type 2 diabetes (Graaf et al., 2016), and several GLP-1 peptide analogs are approved drugs (Gentilella et al., 2019). Alternatively, the development of nonpeptidic small molecule drugs functioning as agonists of GLP-1R remains an elusive goal, despite significant progress being made in recent years (Ma et al., 2020; Zhang et al., 2020). The allosteric nature of GPCRs including GLP-1R and the early discovery of positive allosteric modulators (PAMs) of GLP-1R (Willard et al., 2012) have prompted intensive effort in pursuing GLP-1R PAMs as a novel approach for developing small molecule drugs targeting GLP-1R (Malik & Li, 2021).

2-Aminothiophenes (2-ATs) are small molecule heterocycles (Figure 1, **compound 1**), containing a 5-membered ring core, which are synthetically accessible in good to high yield via variants of the Gewald Reaction (Méndez et al., 2020). 2-AT derivatives have been found to exhibit a diverse array of pharmacological and biological properties. For example, 2-AT-based compounds display anti-cancer (Bozorov et al., 2014), anti-viral (Desantis et al., 2017), antimicrobial (Al-Mousawi et al., 2013), anti-tubercular, and other pharmacologically desirable activities (Scheich et al., 2010; Thanna et al., 2016). For GPCRs, some 2-AT derivatives function as antagonists of the human glucagon receptor (Duffy et al., 2005), whereas a number of others are PAMs of the human adenosine A_1 receptor (Nikolakopoulos et al., 2006). As such, the 2-AT scaffold is present in a large number of thiophene- or aminothiophene-containing drugs (Hartwig et al., 2013) and 2-AT derivatives continue to attract special attention for research and clinical development.

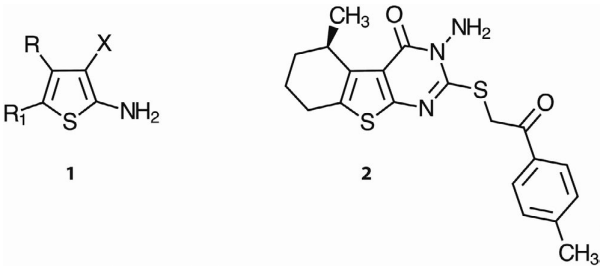

FIGURE 1 Chemical structure of 2-AT (**1**) and **C-1** (**2**)

In our previous work (Redij et al., 2019), we reported a structure-based design approach utilizing the active state structure of GLP-1R (Zhang, Sun, et al., 2017), to screen the ZINC database (Irwin & Shoichet, 2005) in an effort to identify small molecule PAMs as appropriate lead compounds for further drug development. Through in silico screening and in vitro experiment validation, a compound (**C-1**, Figure 1, **compound 2**) with a molecular weight (MW) of 399 g/mol was identified as an ago-PAM of GLP-1R. Subsequent effort to optimize this compound has resulted in the discovery of two novel small molecule 2-AT-based compounds (**S-1** and **S-2)** as potential PAMs of GLP-1R. The **S-1** compound has a MW of 239 g/mol, which is the smallest known PAM of GLP-1R up to now, and satisfies all requirements of Lipinski's rule of five (Lipinski, 2004) as well as Veber's updated rule (Veber et al., 2002) on the number of rotatable bonds. Our work further validates the usefulness of a rational design-based approach in GLP-1R drug discovery, and the reported PAMs have the potential for further drug development.

2 | METHODS

The approach presented here includes several steps: (i) In silico structure-based ligand screening and molecular design; (ii) chemical synthesis of the designed compounds; and (iii) experimental validation of the PAM effects of small molecule compounds.

2.1 | In silico structure-based molecular design

The previously reported compound **C-1** (Redij et al., 2019) was further optimized using the Schrodinger Suite (version 2017). First, the R-groups were generated using Interactive Enumeration Module in the Schrodinger Suite. Next, the chemical structure of the lead compound **C-1** was used as the scaffold, and its H-atoms were replaced by the various R-groups one at a time or in combination. The newly generated compounds were then docked to the same site on the cryo-EM structure of the rabbit GLP-1R (PDB ID: 5VAI) as **C-1** using Glide as described previously (Redij et al., 2019). Briefly, the cryo-EM structure of the rabbit GLP-1R was cropped to retain only its transmembrane domain and was then prepared using Protein Preparation Wizard with default settings. The prepared protein structure was then used to generate the receptor grid around the **C-1** binding site using the Receptor Grid Generation Panel with the default settings. The compounds were prepared using LigPrep module and were docked to the receptor grid

using Glide XP mode and then IFD mode with default settings (Repasky et al., 2012). Top-ranked compounds with the smallest MW were chosen for consideration of synthesis.

2.2 | Medicinal synthesis of newly designed compounds

Chemicals were purchased from Oakwood Products Inc., Sigma Aldrich, TCI America (Portland, OR), and Alfa Aesar. All chemicals were used as purchased. Neither of the active compounds (**S-1** and **S-2**) was identified as PAIN compounds and both show the chemical purity ≥95%.

2.2.1 | Ethyl 2-amino-5-methyl-4,5,6,7-tetrahydro-1-benzothiophene-3-carboxylate (93%) and Ethyl 2-amino-7-methyl-4,5,6,7-tetrahydro-1-benzothiophene-3-carboxylate (7%): **3** (S-1)

To a suspension of 0.96 g (30.0 mM) of sulfur in 5 ml of EtOH, was added 3.2 ml (30.0 mM) of cyanoacetic ethyl ester, and 3.0 ml (25.0 mM) of 3-methylcyclohexanone. The mixture was stirred at room temperature (25°C) for 10 min; After which, 2.6 ml (25.0 mM) of diethylamine was added slowly dropwise over 10 min. The resulting red mixture was stirred overnight at room temperature for 14 h. The mixture was poured into a rapidly stirring beaker of 125 g of ice and 10 ml of water, and the resulting slurry vacuum filtered and rinsed with 3 × 5 ml of ice cold water:ethanol (1:1) to afford 5.0 g of crude **3** (**S-1**). This solid was recrystallized from 40 ml of 1:1 EtOH/H_2O to afford 4.03 g (67.3%) of a 93:7 (5-Me:7-Me) mixture of **3** (**S-1)** as a light yellow solid (Sabnis et al., 1999; Zhang, Luo, et al., 2017). mp 66.5–67.5°C; IR (neat) 3422.80, 3311.02, 3156.93, 3070.54, 2983.94, 2944.78, 2920.90, 2887.82, 2864.48, 2843.98, 1643.57, 1577.06, 1485.95, 1450.98, 1427.88, 1408.35, 1384.35, 1366.57, 1341.40, 1318.50, 1273.38, 1258.70, 1223.00, 1162.25, 1149.42, 1129.64, 1112.88, 1078.42, 1025.81, 984.25, 971.76, 946.18, 934.13, 898.89, 878.02, 816.51, 799.75, 780.49, 765.88, 745.40, 639.46, 627.32, 548.69, 514.80, 464.81, 405.39 cm^{-1}; ^1H NMR (400 MHz, d6-DMSO, 5-Me isomer only) d 7.2 (2H, NH_2, s), 4.15 (2H, -OC$H_2$$CH_3$, m), 2.8 (1H, dd), 2.45 (2H, m), 2.1 (1H, m), 1.7 (2H, m), 1.3 (1H, m), 1.24 (3H, –OCH_2CH_3, t), 0.99 (3H, –CH_3, d); ^1H NMR (400 MHz, $CDCl_3$, 93:7 [5-Me:7-Me major/minor isomer CH_3 chemical shift/integration provided, all rest of peaks provided are of major 5-Me isomer only and integration normalized as though it were isomerically pure]) δ 1.05 (d, J = 6.6 Hz, 2.73H, 5-Me CH_3 major isomer peak), 1.19 (d, J = 6.8 Hz, 0.27H, selected 7-Me CH_3 minor isomer peak), 1.38 (t, J = 3.84 Hz, 3H), 1.42 (m, 1H), 1.77 (m, 2H), 2.18 (qt, Jq =9.8 Hz, Jt = 2.24 Hz, 1H), 2.56 (m, 2H), 2.92 (dd, J = 4.24 Hz, 1H), 4.26 (q, J = 4.6 Hz, 2H), 5.93 (s, 2H); ^{13}C NMR (100 MHz, $CDCl_3$, only data for major 5-Me isomer provided) δ 14.66, 21.91, 24.49, 29.07, 31.53, 35.51, 59.56, 105.85, 117.49, 124.68, 132.66, 162.09; GCMS (5-Me isomer) m/z $(M)^+$ 239.13; GCMS (7-Me isomer) m/z $(M)^+$ 239.15.

2.2.2 | Ethyl 5-methyl-2-{[(methylsulfanyl) carbonothioyl]amino}-4,5,6,7-tetrahydro-1-benzothiophene-3-carboxylate (87%) and Ethyl 7-methyl-2-{[(methylsulfanyl)carbonothioyl] amino}-4,5,6,7-tetrahydro-1-benzothiophene-3-carboxylate (13%): **4**

To a vigorously stirred solution of **3** (**S-1**, 2.25 g, 9.4 mM) in dimethyl sulfoxide (5 ml) at room temperature, was added carbon disulfide (0.94 g, 12.4 mM), followed by concentrated aqueous 20M sodium hydroxide solution (0.600 ml, 12.0 mM). The mixture was allowed to stir for 60 min; after which, dimethyl sulfate (0.94 ml, 9.91 mM) was added dropwise to the reaction mixture while stirring at 5°C. The reaction mixture was then stirred for 2 h and then poured into a beaker of rapidly stirring ice water (125 g ice and 10 ml of water). The resulting slurry was filtered, and the isolated solid was washed with ice cold 30% EtOH/H_2O (2 × 10 ml) and dried under vacuum (1 torr; 50°C; 12 h) to afford 2.83 g (91.3%) of crude **4**. The crude was further purified through recrystallization by dissolving the crude solid in 100 ml of boiling EtOH, followed by the slow addition of 25 ml of boiling water. The mixture was then allowed to slowly cool to room temperature over 1 h, followed by further cooling to 0°C over 30 min. The resulting slurry was filtered, the isolated solid washed with 5 ml of ice cold 15% EtOH/H_2O, and the final pale yellow solid dried under vacuum (75°C; 1 torr) overnite to afford 2.40 g (77.5%) of **4** as a 87:13 5-Me:7-Me mixture of isomers: (Zhang, Luo, et al., 2017) MP 132.5–133.5°C; IR (neat) 3658.11, 2979.53, 2889.02, 2831.93, 1655.67, 1557.56, 1530.07, 1512.94, 1471.58, 1453.79, 1428.09, 1414.82, 1402.55, 1385.03, 1360.77, 1325.08, 1286.19, 1250.99, 1236.15, 1157.59, 1147.53, 1137.30, 1115.35, 1081.66, 1034.85, 1019.40, 998.19, 977.99, 956.66, 908.22, 876.46, 858.71, 783.75, 762.82, 731.22, 691.27, 640.49, 619.11, 581.96, 554.66, 520.99, 435.94 cm^{-1}; ^1H NMR (400 MHz, $CDCl_3$, 93:7 [5-Me:7-Me major/minor isomer NH chemical shift/integration provided, all rest of peaks provided are of major 5-Me isomer only and integration normalized as

though it were isomerically pure]) δ 1.06 (m, 3H), 1.40 (s, 4H), 1.83 (m, 2H), 2.25 (m, 1H), 2.68 (m, 5H), 2.98 (m, 1H), 4.36 (m, 2H), 12.58 (s, 0.13H, NH from 7-methyl isomer); 13.02 (s, 0.87H, NH from 5-methyl isomer); ^{13}C NMR (100 MHz, $CDCl_3$, only data for major 5-Me isomer provided) δ 14.44 (q), 18.60 (q), 21.87 (q), 24.30 (t), 29.08 (d), 31.16 (t), 34.87 (t), 61.08 (t), 112.92 (s), 126.08 (s), 131.10 (s), 150.08 (s), 167.14 (s), 192.49 (s). MS (ESI) calculated for $C_{14}H_{19}NO_2S_3$ 329.1, found 329.2 $[M - H]^+$, found 330.1 $[M + H]^+$.

2.2.3 | 3-amino-6-methyl-2-sulfanyl-5,6,7,8-tetrahydro[1]benzothieno[2,3-*d*]pyrimidin-4(3*H*)-one: **5** (S-2)

A solution of a 87:13 mixture of compound **4**, ethyl 5-methyl-2-(((methylthio)carbonothioyl)amino)-4,5,6,7-tetrahydrobenzo[b]thiophene-3-carboxylate and ethyl 7-methyl-2-(((methylthio)carbono-thioyl)amino)-4,5,6,7-tetrahydrobenzo[b]thiophene-3-carboxylate (2.20 g, 6.68 mM) in ethanol 30 ml was treated with excess 50%–60% grade hydrazine hydrate (3.10 g) and refluxed on a water bath for 14 h. After cooling, the solid obtained was filtered, dried, and washed with 3 × 5 ml of ice-cold ethanol to afford 1.74 g of approximately a 90:10 mixture of crude **5** (**S-2**) and unreacted **4**. The mixture was re-subjected exactly to the above reaction conditions to consume remaining **4**. A total of 1.50 g of crude **4** were obtained. This material was purified to isomerically pure material via recrystallization. The mixture was heated to dissolution in 15 ml DMSO at 70°C for 5 min, followed the addition of 20 ml of 50% EtOH/H_2O at 70°C over 1–2 min and slow cooling to room temperature. The resulting slurry was filtered under vacuum, washed with water (2 × 5 ml), and the resulting white solid dried at 65°C (1 torr) overnite to afford 1.134 g (63.5%) of **S-2** (**5**) as a white powder: (Alagarsamy et al., 2007) MP >220°C (sublimation); IR (neat) 3658.11, 3279.65, 3231.38, 2979.41, 2970.73, 2887.97, 2658.12, 1644.23, 1599.54, 1537.52, 1488.96, 1472.93, 1462.00, 1453.49, 1435.17, 1391.95, 1383.41, 1356.01, 1328.42, 1266.33, 1239.95, 1149.53, 1089.42, 1031.83, 966.85, 946.82, 903.26, 883.08, 870.46, 811.04, 786.61, 762.26, 695.62, 665.48, 652.07, 626.73, 559.37, 526.18, 511.57, 489.72, 474.01, 452.92, 444.67, 435.80, 427.56 cm^{-1}; ^{1}H NMR (hydrate form, 400 MHz, DMSO-d_6) δ 1.03 (d, J = 6.44 Hz, 3H), 1.38 (m, 1H), 1.81 (m, 2H), 2.23 (dd, J = 10.0, 7.4 Hz, 1H), 2.62 (m, 2H), 3.06 (dd, J = 13.0, 4.0 Hz, 1H), 5.74 (s, 1H), 6.38 (s, 1H), 7.03 (s, 1H); ^{13}C NMR (100 MHz, DMSO-d_6) δ 21.51 (q), 24.13 (t), 28.10 (d), 30.86 (t), 33.55 (t), 113.98 (s), 124.88 (s), 129.62 (s), 154.45 (s), 159.50 (s), 167.87 (s). MS (ESI) calculated for $C_{11}H_{13}N_3OS_2$ 267.1, found 266.2 $[M - H]^+$, found 268.1 $[M + H]^+$.

2.2.4 | 4-{[(3-amino-6-methyl-4-oxo-3,4,5,6,7,8-hexahydro[1]benzothieno[2,3-*d*]pyrimidin-2-yl)sulfanyl]-acetyl}benzonitrile: **6**

A mixture of 0.500 g (0.002 mol) of 3-amino-2-mercapto-5-methyl-5,6,7,8-tetrahydro-benzo[4,5]thieno[2,3-d]pyrimidin-4(3H)-one (**5**/**S-2**), 0.002 mol of 4-(2-bromoacetyl)benzonitrile, and 0.0025 mol of sodium acetate in 10 ml of methanol was refluxed for 8 h. The reaction mixture was allowed to cool to room temperature, the resulting slurry was vacuum filtered, and the isolated solid washed with ethanol, and dried under vacuum. The filtrate of **6** (70% yield) was obtained as a white solid (Ashalatha et al., 2007). Selected ^{1}H NMR data only: ^{1}H NMR (400 MHz, DMSO-d_6): 1.0 (d, 3H, –CH_3), 1.4 (m, 1H), 1.8 (m, 2H), 2.4 (s, 3H, CH_3-Ar, s), 2.65 (m, 2H), 3.05 (dd, 1H), 4.6 (s, 1H), 5.8 (s, 2H, NH_2), 8.1 (d, 2H, H-Ar), 8.2 (d, 2H, H-Ar).

2.3 | In vitro testing of potential GLP-1R PAMs

2.3.1 | Biological materials

HEK293 cell stably expressing CRE/CREB luciferase reporter gene (BPS Bioscience #60515), RPMI medium (Corning #10-040), Krebs-Ringer Solution, HEPES-buffered (Alfa Aesar #J67795-K2), L-Glutamine (Gibco #25030-081), HEPES (Gibco #15630-080), Sodium Pyruvate (Gibco #11360-070), β-mercaptoethanol (MP #806444), D-Glucose (#G-7528), Fetal Bovine Serum (Fisher #03600511), penicillin/streptomycin (Corning #30-002-Cl), Hygromycin B (Alfa Aesar #J60681), Lipofectamine 2000 (Invitrogen #11668027), vasoactive intestinal peptide receptor (VIPR) peptide agonist (Sigma #V3628), VIPR peptide antagonist (Sigma #SCP0260), GLP-1R peptide agonist (Sigma #9416), 6-well cell culture plates (Ultra Cruz #sc-204443), 96-well cell culture plates (Sigma #CLS9102), Luciferase cell culture lysis reagent (Promega #E1531), Luciferase assay reagent (Promega #E1501), and Ultra-Sensitive Rat Insulin Kit (Crystal Chem #90060) were purchased from vendors. VIPR1 receptor plasmid (#51865) was purchased from Addgene, Flag-tagged Human GLP-1R and Flag-tagged pCMV-N-Flag negative control vector were purchased from vendors (Sino Biological Inc. #HG13944-NF and #CV061) and INS-1 832/13 cells were provided by Dr. Xianxin Hua at Perelman School of Medicine, Pfu DNA polymerase kit (Thermofisher #EP0501) and primers (University of Pennsylvania) were purchased from vendors.

2.3.2 | Transfection and cell culture

HEK293 cells stably expressing CRE/CREB Reporter (luciferase) were cultured in RPMI medium supplemented with 8% (v/v) fetal bovine serum, 2% (v/v) penicillin/streptomycin, and 100 μg/ml of Hygromycin B. Cells were maintained in an incubator at 37°C with 5% CO_2. Cells were seeded into 6-well cell culture plates 1 day before transfection. After overnight incubation, one well of cell was transiently transfected with 3.4 μg of human GLP-1R or empty vector, respectively, using lipofectamine 2000. After 4 h of transfection, transfection medium was replaced by RPMI medium supplemented with 5% (v/v) fetal bovine serum and 2% (v/v) penicillin/streptomycin. After 24 h of incubation, cells were trypsinized and seeded into 96-well cell culture plates (5.5×10^4 cells/well) and maintained at 37°C in 5% CO_2 incubator for 24 h. The cells were starved using RPMI with 0.5% sera. After 24 h of starvation, the transfected cells were treated with compounds as indicated.

2.3.3 | Luciferase assay

Compounds dissolved in 100% DMSO were diluted to indicated concentration in RPMI 1640 (0.5% DMSO included for all cell culture). After 4 h of treatment, cells were harvested by cold luciferase cell culture lysis buffer and kept on shaker for 10 min at 4°C. Luciferase activity was measured using luciferin substrate, and luminescence was read by Wallac 1420 multiplate reader. Luciferase activity of HEK293 reporting cells cultured using 0.5% DMSO and full RPMI medium was used as a vehicle control. Protein concentration of each well was determined by Bradford assay.

First, all compounds were tested at one or two random concentrations to determine their activity as an ago-agonist. If a compound showed even low activity, it was chosen for synergistic study. To determine the final concentration of the compound for the synergistic study, a rough dose curve with GLP-1 and varied compound concentration was generated and the final concentration of the compound was chosen based on the curve.

2.3.4 | Non-specific effect of GLP-1R PAM on VIPR1

HEK293 cells stably expressing CRE/CREB Reporter (luciferase) were cultured in RPMI 1640 supplemented with 8% (v/v) fetal bovine serum, 2% (v/v) penicillin/streptomycin, and 100 μg/ml of Hygromycin B. Cells were maintained at 37°C with 5% CO_2. Cells were seeded into 6-well cell culture plates 1 day before transfection. After overnight incubation, cells were transiently transfected with 3.4 μg of VIPR1, using Lipofectamine 2000. After 4 h of transfection, medium was replaced by RPMI supplemented with 5% (v/v) fetal bovine serum. After 24 h of incubation, cells were trypsinized and seeded into 96-well cell culture plates (5.5×10^4 cells/well) and maintained at 37°C in 5% CO_2 for 24 h. After 24 h of incubation, the cells were starved with RPMI with 0.5% sera. After 24 h of starvation, the transfected cells were treated with compounds as indicated.

2.3.5 | Glucose stimulated insulin secretion in INS-1 832/13 cells

INS-1 832/13 cells were cultured in RPMI 1640 supplemented with 2 mM L-glutamine, 1 mM sodium pyruvate, 10% FBS, 10 mM HEPES, 100 units/ml penicillin, 100 μg/ml streptomycin, and 50 μM β-mercaptoethanol. Cells were maintained in an incubator at 37°C with 5% CO_2. To determine the effect of GLP-1R PAM **S-1** on insulin secretion, INS-1 cells were seeded onto six-well plates, 10^6 cells/well. After 48 h of incubation, cells were washed twice with 500 μl of Krebs–Ringer Solution, HEPES-buffered (KRB) and starved for 2 h in fresh KRB supplemented with 0.1% serum. After 2 h of starvation, the buffer was replaced with 1 ml of KRB containing 0.1% serum, 16.7 mM glucose and 5 μM of **S-1**, or 181 nM of GLP-1 with 0.05% DMSO or 0.05% DMSO alone (vehicle control) and incubated at 37°C with 5% CO_2. After 90 min, the supernatant was collected, centrifuged at 100 x *g* for 5 min at 4°C, and aliquoted and stored at −20°C. These samples were used to determine insulin concentration using insulin detection kit ELISA following the manual.

2.3.6 | Data analysis

The concentration-dependent dose–response curve was generated using Graph Pad Prism 6.0 for Mac (GraphPad Software Inc.). The curves were fitted based on sigmoidal dose response with the bottom parameter being kept 0. The EC_{50} value was calculated from Prism. The statistical difference between different groups was analyzed by two-way ANOVA module in Prism.

2.4 | Mechanistic studies

2.4.1 | Protein detection by western blotting

INS-1 cells were collected and lysed with RIPA lysis buffer (Sigma) containing protease and phosphatase inhibitors.

Protein concentrations were determined using a BCA assay kit (Thermo Scientific). Cell lysates were subjected to polyacrylamide gel electrophoresis on Novex gels (Life Technologies), and protein was transferred to PVDF membranes (Life Technologies). Blocking was performed in TBST containing 5% non-fat dry milk or 3% BSA based on the manufacturer's blocking instructions. Antibody against p-Creb (#L0915) was purchased from Santa Cruz Biotechnology. Antibody against Creb (#9197) was purchased from Cell Signaling Technology. Antibody against actin (#A5441) was purchased from Sigma. Anti-rabbit and anti-mouse secondary antibodies labeled with HRP were purchased from Bio-Rad. The proteins were visualized by detection with Amersham ECL Western blotting detection reagents (GE Healthcare).

2.4.2 | Docking studies of compounds **S-1** and **S-2**

Compounds **S-1** and **S-2** were docked, respectively, to the same site on the cryo-EM structure of the rabbit GLP-1R (PDB ID: 5VAI) as **C-1** using the same parameters and procedures as described above.

3 | RESULTS

3.1 | Synthesis of 2-aminothiophene derivatives

After the discovery of the compound **C-1** as an ago-PAM of GLP-1R (Redij et al., 2019), we subsequently attempted to further improve its binding affinity using computer-aided drug design (CADD) techniques. The H-atoms at different positions of **C-1** were systematically replaced with various functional groups virtually (Figure S1), and the modified compounds were subsequently docked into the same binding site on GLP-1R as **C-1** (Table S1). Based on the docking score and synthetic feasibility, several compounds with the same scaffold were eventually synthesized following the route as shown in Scheme 1 (Figure S2).

All intermediates and final products were tested in vitro for their allosteric activity on human GLP-1R using luciferase-based reporter gene assay.

3.2 | In vitro activity of the synthesized compounds

Of all the intermediates and final products tested, two intermediates (**3**, **S-1** and **5**, **S-2**) were found to be the PAMs of GLP-1R (Figure 2). The activation of GLP-1R by different concentrations of GLP-1 (0.014 nM-145 nM) in combination with **S-1** (23.5 μM) or **S-2** (71 μM), respectively, was studied by luciferase activity responding to cAMP production using HEK293-CREB cells transiently expressing human GLP-1R. GLP-1R activity stimulated by GLP-1 in combination with **S-1** (23.5 μM) or **S-2** (71 μM), respectively, was significantly increased than using GLP-1 alone and the allosteric effect was dose dependent.

3.3 | Compound S-1 does not stimulate VIPR1 activity

Besides GLP-1R, the HEK293 cells are known to express other functional Class B GPCRs including VIPR1

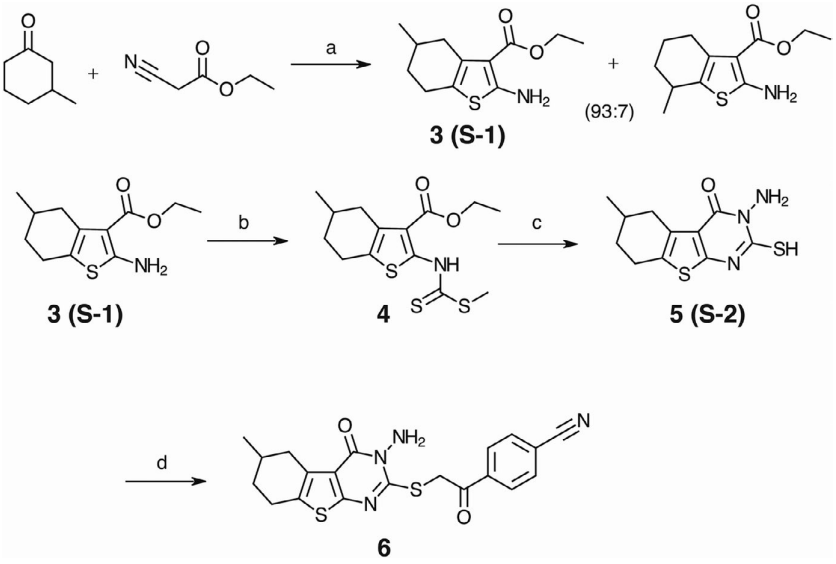

SCHEME 1 General synthetic scheme for substituted 3-amino-8-methyl-2-((2-oxo-2-phenylethyl)thio)-5,6,7,8-tetrahydrobenzo[4,5]thieno[2,3-*d*]pyrimidin-4(3*H*)-one[a]. [a]Reagents and conditions (a) S, DEA, ETOH, 25°C, 12 h; (b) NaOH, CS_2, DMS, DMSO, 25°C, 12 h; (c) hydrazine hydrate (50–60%), MeOH, 25°C, 8 h; (d) substituted 2-bromo-1-phenylethan-1-one, MeOH, reflux, 8 h

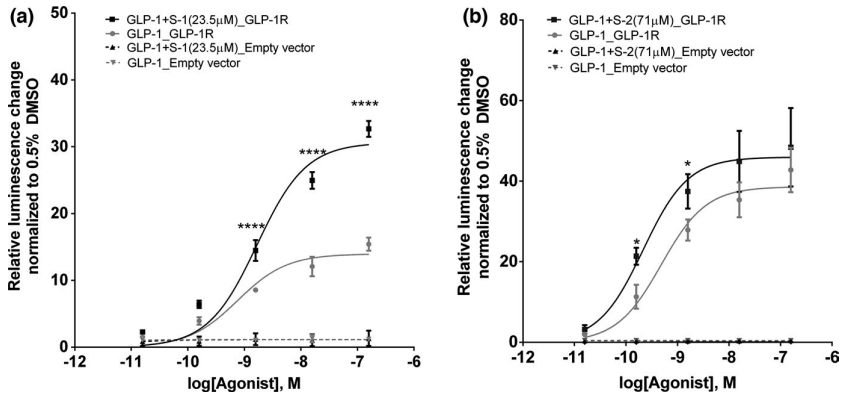

FIGURE 2 Potential allosteric effect of **S-1** and **S-2** on human GLP-1R. (a) The effect of GLP-1 on HEK293 cells expressing human GLP-1R or empty vector in the presence or absence of **S-1** (23.5 μM). (b) The effect of GLP-1 on HEK293 cells expressing human GLP-1R or empty vector in the presence or absence of **S-2** (71 μM). GLP-1R activation was assessed as luminescence normalized to protein concentration and plotted as luminescence fold change with respect to vehicle control (0.5% DMSO). Data are average of three independent experiments with at least three technical replicates for each conditions, and error bars for each concentration were plotted as SEM ($n = 3$). Statistical analysis was done using 2-way ANOVA (****$p < 0.0001$; **$p < 0.001$; *$p < 0.5$). The comparison is done between the data points of the dose–response curve generated due to GLP-1's effect on GLP-1R in the presence and absence of **S-1** or **S-2**

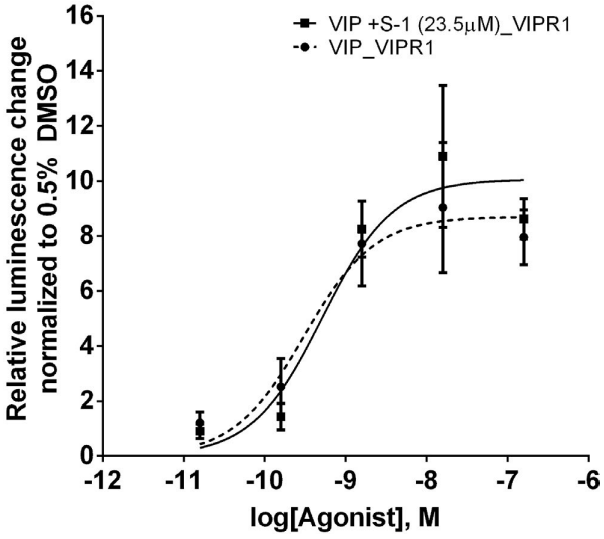

FIGURE 3 Potential non-specific activity of compound **S-1** on VIPR1. VIPR1 activation was assessed as luminescence normalized to protein concentration and plotted as luminescence fold change with respect to vehicle control (0.5% DMSO). Data shown are average of three independent experiments with at least three technical replicates for each conditions, and error bars for each concentration were plotted as SEM ($n = 3$). Statistical analysis was done using 2-way ANOVA. The comparison was done between the corresponding data points on the two dose–response curve generated due to the effect of GLP-1 alone and in combination with **S-1**

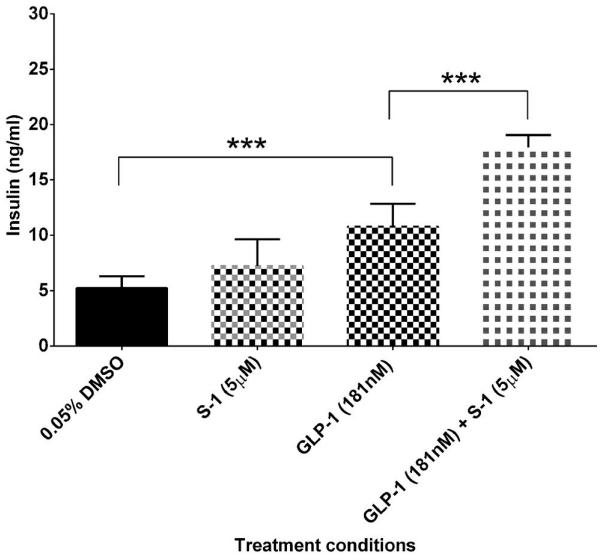

FIGURE 4 Glucose stimulated insulin production induced by GLP-1 and **S-1** in INS-1 832/13 cells. INS-1 832/13 cells were treated with GLP-1 (181 nM) and **S-1** (5 μM) in the presence of 16.7 mM glucose after 2 h of starvation with KRB buffer. Data shown are average of four independent experiments, and error bars for each concentration were plotted as SEM ($n = 4$) Statistical analysis was done using two-way ANOVA (****$p < 0.0001$)

(Atwood et al., 2011). Since **S-1** is more stable and potent, its behavior (23.5 μM) on VIPR1 in the presence of VIPR peptide agonist (0.014 nM-145 nM) was studied using the same cell line with overexpressed VIPR1. The VIPR1 activity in response to VIPR agonist in combination with **S-1** was similar to that using VIPR agonist alone, indicating that **S-1** showed no specific activity on VIPR1 (Figure 3).

3.4 | S-1 Stimulates insulin secretion

The insulin production activity of **S-1** was assessed by in vitro insulin secretion assay in INS-1 832/13 cells. The results indicate that no significant difference was observed between the amount of insulin produced by vehicle control and **S-1** (5 μM). It is of interest to note, however, that in combination with GLP-1, **S-1** can stimulate insulin secretion more than 1.5-fold more than GLP-1 alone in the presence of 16.7 mM of glucose (Figure 4). Thus, these data indicate that **S-1** can enhance glucose-dependent insulin production in GLP-1R expressed cells and may even improve GLP-1's efficacy enough to have potential clinical ramifications.

3.5 | Mechanism of action of compound S-1 in INS-1 cells

The phosphorylation at Ser133 of CREB, a downstream target of cAMP/PKA, can be induced by GLP-1 in INS-1 cells, which promotes insulin transcription (Skoglund et al., 2000; Sonoda et al., 2008). Given the increased insulin secretion in INS-1 cells with GLP-1 and **S-1** co-treatment relative to GLP-1or **S-1** treatment alone (Figure 4), the synergistic effect of **S-1** with GLP-1 treatment may be partly due to the enhanced impact on CREB phosphorylation. To this end, GLP-1and **S-1** were used to treat INS-1 cells either combined together or separately for 10 min. The phosphorylated CREB level in INS-1 cells co-treated with GLP-1 and **S-1** (Figure 5a, Lane 4) is higher than with GLP-1 or **S-1** treatment alone (Figure 5a, Lane 2 or 3). This conclusion was confirmed by quantifying the intensity of the bands using Image J software (Figure 5b).

Docking studies showed that the docking score of compounds **S-1** (−7.9 kcal/mol) and **S-2** (−8.1 kcal/mol) was much worse than compound **6** (−11.2 kcal/mol). Despite the inaccuracy of the scoring function, a likely reason for this discrepancy is that compounds **S-1** and **S-2** bound to a different active conformation of GLP-1R from compound **6**. More experiments are needed to confirm this.

4 | DISCUSSION

The development of GLP-1R PAMs as small molecule drugs could offer reduced side effects as a therapeutic benefit (Khoury et al., 2014; Pupo et al., 2016; Wootten et al., 2017) and has attracted considerable effort toward the early discovery of GLP-1R PAMs worldwide (Chen et al., 2007; Teng et al., 2007). Our previous structure-based design effort (Redij et al., 2019) using the cryo-EM structure of the GLP-1R in its active state (Zhang, Sun, et al., 2017) for in silico screening resulted in the identification of one lead compound (**C-1**) as an ago-PAM of GLP-1R. Subsequently, we carried out structure-based lead optimization in conjunction with 2-AT analogue synthesis which has led to the discovery of two novel small molecule PAMs (**S-1** and **S-2**). The synergistic effect of **S-1** was further confirmed by insulin secretion experiments, and the initial mechanistic studies suggest **S-1** induces increased CREB phosphorylation.

Interestingly, compounds **S-1** and **S-2** share the common 2-AT scaffold (Figure 1) and are the smallest known PAMs of GLP-1R. Further, the compound **S-1** completely meets Lipinski's Rule of Five (Lipinski, 2004) and Veber's corollary rules (Veber et al., 2002). In addition, when applied in combination with GLP-1 in HEK293 cells overexpressed VIPR1, **S-1** did not induce non-specific activity on this

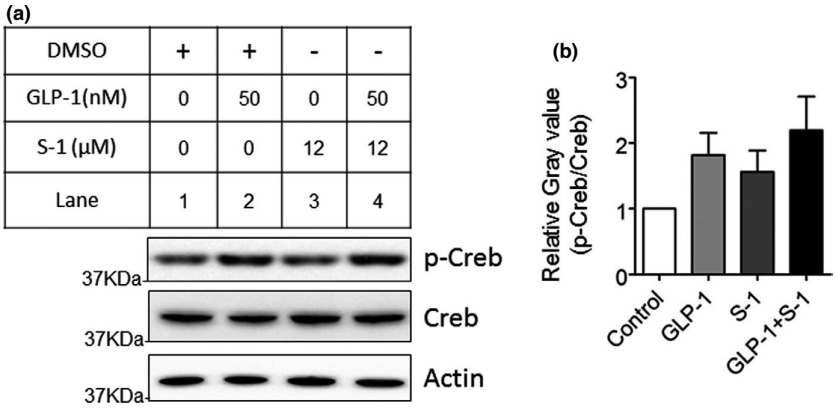

FIGURE 5 Synergy effect of GLP-1 and **S-1** co-treatment on INS-1 cells to stimulate CREB Ser133 phosphorylation. (a) INS-1 cells were plated in six-well plates at a density of 2×10^5 cells per well. Twenty-4 h later, the cell culture medium was removed and replaced with a serum-free cell culture medium. After an overnight (16 h) starvation, the cells were treated using drugs (i.e., GLP-1, 50 nM; **S-1**, 12 μM) for 10 min. Then, the cells were selected and lysed to detect phosphorylated Creb level using WB assay. (b) The quantification of Western blot results was done using Image J software

receptor (Figure 3). Given its favorable pharmacological properties, the 2-AT-based scaffold demonstrated specificity toward GLP-1R and excellent capability in stimulating insulin secretion (Figure 4). Thus, compound **S-1** has emerged as an excellent lead compound for further drug discovery effort. Currently, we are engaging in structure-based synthetic efforts to chemically modify **S-1** to further increase potency and improve specificity to GLP-1R.

It should be noted that both **S-1** and **S-2** are intermediates in the synthesis of compound **6** and none of the designed compounds chosen for testing showed activity toward GLP-1R. There are several reasons that could be behind this structure-based design failure. The scoring function used to rank the designed compounds is not completely reliable. The binding conformation of compound **C-1** adopted for structure-based optimization is likely not correct. Third, the conformational change of GLP-1R triggered by the binding of various ligands might not be sampled completely during the optimization process. Fourth, the docking score was based on our understanding of protein–ligand interactions and the impact of solvents. It represents the protein-level prediction of ligand activity, while the assays used in this work are cell-based. There are much more variables inside the cells that could affect the assay results. All these factors could affect the accuracy of the estimated binding affinity of various compounds.

Surprisingly, the docking scores of compounds **S-1** and **S-2** are much worse than that of compound **6**. Besides factors mentioned above that could affect the inaccuracy of the scoring function, we think another factor contributing to this discrepancy is that compounds **S-1** and **S-2** likely bound to a different active conformation of GLP-1R from compound **6**. Clearly, more experiments are needed to confirm this. It will be of interest to elucidate the binding mode of **S-1** and **S-2** for future structure-based lead optimization efforts.

5 | CONCLUSIONS

To develop novel small molecule PAMs of GLP-1R for the treatment of type 2 diabetes, we have discovered two 2-AT derivatives that bind to GLP-1R specifically and increase insulin secretion of GLP-1R significantly in the presence of the GLP-1 peptide agonist. Mechanistically the synergistic effect of these compounds is possibly due to the enhanced impact on CREB phosphorylation. Docking studies suggested that these compounds likely bind to a different active conformation of GLP-1R from the initial lead compound. These 2-AT derivatives are easy to synthesize and have favorable pharmacological properties. Their chemical structures are distinct from other known PAMs. Hence, 2-AT derivatives represent a new and promising class of GLP-1R PAMs with great potential for further drug development.

ACKNOWLEDGEMENTS

The authors thank Mr. Faisal Malik at Dr. Zhijun Li's laboratory for help with the docking studies. This work was supported in part by the Institute for Translational Medicine and Therapeutics (ITMAT) Transdisciplinary Program in Translational Medicine and Therapeutics at University of Pennsylvania and in part by the National Institute of General Medical Sciences of the National Institutes of Health under Award Number R15GM140406. The content is solely the responsibility of the authors and does not necessarily represent the official views of the National Institutes of Health.

DATA AVAILABILITY STATEMENT

All the data generated are included in the manuscript or available by contacting the corresponding author.

REFERENCES

Alagarsamy, V., Solomon, V. R., Deepa, G., Parthiban, P., & Anjana, G. V. (2007). Synthesis and pharmacological investigation of 3-subsituted-amino-2-methylsulfanyl-5,6,7,8-tetrahydro-3H-benzo[4,5]thieno[2,3-d]pyrimidin-4-ones as analgesic and anti-inflammatory agents. *Archiv der Pharmazie*, *340*(7), 352–358. https://doi.org/10.1002/ardp.200700017

Al-Mousawi, S. M., El-Apasery, M. A., & Mahmoud, H. M. (2013). Disperse dyes based on aminothiophenes: Their dyeing applications on polyester fabrics and their antimicrobial activity. *Molecules*, *18*(6), 7081–7092.

Ashalatha, B. V., Narayana, B., Vijaya Raj, K. K., & Suchetha Kumari, N. (2007). Synthesis of some new bioactive 3-amino-2-mercapto-5,6,7,8-tetrahydro[1]benzothieno[2,3-d]pyrimidin-4(3H)-one derivatives. *European Journal of Medicinal Chemistry*, *42*(5), 719–728.

Atwood, B. K., Lopez, J., Wager-Miller, J., Mackie, K., & Straiker, A. (2011). Expression of G protein-coupled receptors and related proteins in HEK293, AtT20, BV2, and N18 cell lines as revealed by microarray analysis. *BMC Genomics*, *12*, 14. https://doi.org/10.1186/1471-2164-12-14

Bozorov, K., Ma, H.-R., Zhao, J.-Y., Zhao, H.-Q., Chen, H., Bobakulov, K., Xin, X.-L., Elmuradov, B., Shakhidoyatov, K., & Aisa, H. A. (2014). Discovery of diethyl 2,5-diaminothiophene-3,4-dicarboxylate derivatives as potent anticancer and antimicrobial agents and screening of anti-diabetic activity: Synthesis and in vitro biological evaluation. Part 1. *European Journal of Medicinal Chemistry*, *84*, 739–745.

Chen, D., Liao, J., Li, N., Zhou, C., Liu, Q., Wang, G., Zhang, R., Zhang, S., Lin, L., Chen, K., Xie, X., Nan, F., Young, A. A., & Wang, M. W. (2007). A nonpeptidic agonist of glucagon-like peptide 1 receptors with efficacy in diabetic Db/Db mice. *Proceedings of the National Academy of Sciences of the United States of America*, *104*(3), 943–948.

Desantis, J., Nannetti, G., Massari, S., Barreca, M. L., Manfroni, G., Cecchetti, V., Palù, G., Goracci, L., Loregian, A., & Tabarrini, O. (2017). Exploring the cycloheptathiophene-3-carboxamide scaffold to disrupt the interactions of the influenza polymerase

subunits and obtain potent anti-influenza activity. *European Journal of Medicinal Chemistry*, *138*, 128–139.

Duffy, J. L., Kirk, B. A., Konteatis, Z., Campbell, E. L., Liang, R., Brady, E. J., Candelore, M. R., Ding, V. D. H., Jiang, G., Liu, F., Qureshi, S. A., Saperstein, R., Szalkowski, D., Tong, S., Tota, L. M., Xie, D., Yang, X., Zafian, P., Zheng, S., … Tata, J. R. (2005). Discovery and investigation of a novel class of thiophene-derived antagonists of the human glucagon receptor. *Bioorganic & Medicinal Chemistry Letters*, *15*(5), 1401–1405.

Gentilella, R., Pechtner, V., Corcos, A., & Consoli, A. (2019). Glucagon-like peptide-1 receptor agonists in type 2 diabetes treatment: Are they all the same? *Diabetes/metabolism Research and Reviews*, *35*(1), e3070.

Graaf, C., de Donnelly, D., Wootten, D., Lau, J., Sexton, P. M., Miller, L. J., Ahn, J.-M., Liao, J., Fletcher, M. M., Yang, D., Brown, A. J. H., Zhou, C., Deng, J., & Wang, M.-W. (2016). Glucagon-like peptide-1 and its class B G protein-coupled receptors: A long march to therapeutic successes. *Pharmacological Reviews*, *68*(4), 954–1013.

Hartwig, J., Ceylan, S., Kupracz, L., Coutable, L., & Kirschning, A. (2013). Heating under high-frequency inductive conditions: Application to the continuous synthesis of the neurolepticum olanzapine (Zyprexa). *Angewandte Chemie (International Ed. in English)*, *52*(37), 9813–9817.

Irwin, J. J., & Shoichet, B. K. (2005). ZINC–a free database of commercially available compounds for virtual screening. *Journal of Chemical Information and Modeling*, *45*(1), 177–182.

Khoury, E., Clement, S., & Laporte, S. A. (2014). Allosteric and biased g protein-coupled receptor signaling regulation: Potentials for new therapeutics. *Frontiers in Endocrinology*, *5*, 68.

Koole, C., Pabreja, K., Savage, E. E., Wootten, D., Furness, S. G., Miller, L. J., Christopoulos, A., & Sexton, P. M. (2013). Recent advances in understanding GLP-1R (glucagon-like peptide-1 receptor) function. *Biochemical Society Transactions*, *41*(1), 172–179.

Lipinski, C. A. (2004). Lead- and drug-like compounds: The rule-of-five revolution. *Drug Discovery Today: Technologies*, *1*(4), 337–341.

Ma, H., Huang, W., Wang, X., Zhao, L., Jiang, Y., Liu, F., Guo, W., Sun, X., Zhong, W., Yuan, D., & Xu, H. E. (2020). Structural insights into the activation of GLP-1R by a small molecule agonist. *Cell Research*, *30*(12), 1140–1142.

Malik, F., & Li, Z. (2021). Non-peptide agonists and positive allosteric modulators of glucagon-like peptide-1 receptors: Alternative approaches for treatment of type 2 diabetes. *British Journal of Pharmacology*, *179*(4), 511–525. https://doi.org/10.1111/bph.15446

Méndez, M., Matter, H., Defossa, E., Kurz, M., Lebreton, S., Li, Z., Lohmann, M., Löhn, M., Mors, H., Podeschwa, M., Rackelmann, N., Riedel, J., Safar, P., Thorpe, D. S., Schäfer, M., Weitz, D., & Breitschopf, K. (2020). Design, synthesis, and pharmacological evaluation of potent positive allosteric modulators of the glucagon-like peptide-1 receptor (GLP-1R). *Journal of Medicinal Chemistry*, *63*(5), 2292–2307.

Nikolakopoulos, G., Figler, H., Linden, J., & Scammells, P. J. (2006). 2-Aminothiophene-3-carboxylates and carboxamides as adenosine A1 receptor allosteric enhancers. *Bioorganic & Medicinal Chemistry*, *14*(7), 2358–2365.

Pupo, A. S., Duarte, D. A., Lima, V., Teixeira, L. B., Parreiras-e-Silva, L. T., & Costa-Neto, C. M. (2016). Recent updates on GPCR biased agonism. *Pharmacological Research*, *112*, 49–57.

Redij, T., Ma, J., Li, Z., Hua, X., & Li, Z. (2019). Discovery of a potential positive allosteric modulator of glucagon-like peptide 1 receptor through virtual screening and experimental study. *Journal of Computer-Aided Molecular Design*, *33*(11), 973–981.

Repasky, M. P., Murphy, R. B., Banks, J. L., Greenwood, J. R., Tubert-Brohman, I., Bhat, S., & Friesner, R. A. (2012). Docking performance of the glide program as evaluated on the astex and DUD datasets: A complete set of glide SP results and selected results for a new scoring function integrating WaterMap and glide. *Journal of Computer-Aided Molecular Design*, *26*(6), 787–799.

Sabnis, R., Rangnekar, D., & Sonawane, N. (1999). 2-Aminothiophenes by the Gewald reaction. *Journal of Heterocyclic Chemistry*, *36*, 333–345.

Scheich, C., Puetter, V., & Schade, M. (2010). Novel small molecule inhibitors of MDR *Mycobacterium tuberculosis* by NMR fragment screening of antigen 85C. *Journal of Medicinal Chemistry*, *53*(23), 8362–8367.

Skoglund, G., Hussain, M. A., & Holz, G. G. (2000). Glucagon-like peptide 1 stimulates insulin gene promoter activity by protein kinase A-independent activation of the rat insulin I gene CAMP response element. *Diabetes*, *49*(7), 1156–1164. https://doi.org/10.2337/diabetes.49.7.1156

Sonoda, N., Imamura, T., Yoshizaki, T., Babendure, J. L., Lu, J.-C., & Olefsky, J. M. (2008). Beta-arrestin-1 mediates glucagon-like peptide-1 signaling to insulin secretion in cultured pancreatic beta cells. *Proceedings of the National Academy of Sciences of the United States of America*, *105*(18), 6614–6619.

Teng, M., Johnson, M. D., Thomas, C., Kiel, D., Lakis, J. N., Kercher, T., Aytes, S., Kostrowicki, J., Bhumralkar, D., Truesdale, L., May, J., Sidelman, U., Kodra, J. T., Jørgensen, A. S., Olesen, P. H., de Jong, J. C., Madsen, P., Behrens, C., Pettersson, I., … Lau, J. (2007). Small molecule ago-allosteric modulators of the human glucagon-like peptide-1 (HGLP-1) receptor. *Bioorganic & Medicinal Chemistry Letters*, *17*(19), 5472–5478.

Thanna, S., Knudson, S. E., Grzegorzewicz, A., Kapil, S., Goins, C. M., Ronning, D. R., Jackson, M., Slayden, R. A., & Sucheck, S. J. (2016). Synthesis and evaluation of new 2-aminothiophenes against *Mycobacterium tuberculosis*. *Organic & Biomolecular Chemistry*, *14*(25), 6119–6133.

Veber, D. F., Johnson, S. R., Cheng, H. Y., Smith, B. R., Ward, K. W., & Kopple, K. D. (2002). Molecular properties that influence the oral bioavailability of drug candidates. *Journal of Medicinal Chemistry*, *45*(12), 2615–2623.

Willard, F. S., Bueno, A. B., & Sloop, K. W. (2012). Small molecule drug discovery at the glucagon-like peptide-1 receptor. *Experimental Diabetes Research*, *2012*, 1–9.

Wootten, D., Miller, L. J., Koole, C., Christopoulos, A., & Sexton, P. M. (2017). Allostery and biased agonism at class B G protein-coupled receptors. *Chemical Reviews*, *117*(1), 111–138.

Zhang, X., Belousoff, M. J., Zhao, P., Kooistra, A. J., Truong, T. T., Ang, S. Y., Underwood, C. R., Egebjerg, T., Šenel, P., Stewart, G. D., Liang, Y.-L., Glukhova, A., Venugopal, H., Christopoulos, A., Furness, S. G. B., Miller, L. J., Reedtz-Runge, S., Langmead, C. J., Gloriam, D. E., … Wootten, D. (2020). Differential GLP-1R binding and activation by peptide and non-peptide agonists. *Molecular Cell*, *80*(3), 485–500. https://doi.org/10.1016/j.molcel.2020.09.020

Zhang, Y., Luo, L., Han, C., Lv, H., Chen, D., Shen, G., Wu, K., Pan, S., & Ye, F. (2017). Design, synthesis, and biological activity of tetrahydrobenzo[4,5]Thieno[2,3-d]pyrimidine derivatives as anti-inflammatory agents. *Molecules*, *22*(11), E1960.

Zhang, Y., Sun, B., Feng, D., Hu, H., Chu, M., Qu, Q., Tarrasch, J. T., Li, S., Sun Kobilka, T., Kobilka, B. K., & Skiniotis, G. (2017). Cryo-EM structure of the activated GLP-1 receptor in complex with a G protein. *Nature*, *546*(7657), 248–253.

SUPPORTING INFORMATION

Additional supporting information may be found in the online version of the article at the publisher's website.

How to cite this article: Redij, T., McKee, J. A., Do, P., Campbell, J. A., Ma, J., Li, Z., Miller, N., Srikanlaya, C., Zhang, D., Hua, X., & Li, Z. (2022). 2-Aminothiophene derivatives as a new class of positive allosteric modulators of glucagon-like peptide 1 receptor. *Chemical Biology & Drug Design*, *00*, 1–11. https://doi.org/10.1111/cbdd.14039